



Pressure-induced polarization reversal in multiferroic YMn_2O_5

Rajit P. Chaudhury,¹ Clarina R. dela Cruz,^{2,3} Bernd Lorenz,¹ Yanyi Sun,¹ Ching-Wu Chu,^{1,4,5} S. Park,⁶ and Sang-W. Cheong⁶

¹*Department of Physics and TCSUH, University of Houston, Houston, Texas 77204, USA*

²*Department of Physics and Astronomy, University of Tennessee, Knoxville, Tennessee 37996, USA*

³*Oak Ridge National Laboratory, Oak Ridge, Tennessee 37831, USA*

⁴*Lawrence Berkeley National Laboratory, 1 Cyclotron Road, Berkeley, California 94720, USA*

⁵*Hong Kong University of Science and Technology, Hong Kong, China*

⁶*Rutgers Center for Emergent Materials and Department of Physics and Astronomy, Rutgers University, Piscataway, New Jersey 08854, USA*

(Received 7 May 2008; revised manuscript received 31 May 2008; published 24 June 2008)

The low-temperature ferroelectric polarization of multiferroic YMn_2O_5 is completely reversed at a critical pressure of 10 kbar and the phase transition from the incommensurate to the commensurate magnetic phase is induced by pressures above 14 kbar. The high-pressure data correlate with thermal-expansion measurements, indicating a significant lattice strain at the low-temperature transition into the incommensurate phase. The results support the exchange striction model for the ferroelectricity in multiferroic RMn_2O_5 compounds and they show the importance of magnetic frustration as well as the spin-lattice coupling.

DOI: [10.1103/PhysRevB.77.220104](https://doi.org/10.1103/PhysRevB.77.220104)

PACS number(s): 77.80.-e, 75.30.-m, 75.50.Ee, 77.84.Bw

Multiferroic magnetoelectric compounds in which ferroelectricity and magnetic order coexist and mutually interact have been in the focus of attention very recently because of a wealth of novel physical phenomena observed in these complex materials.¹⁻⁴ Among the family of multiferroics, the RMn_2O_5 (R = rare earth, Y, Bi) manganites are of significant interest because of their extreme complexity with transitions between different commensurate magnetic structures (CM) and incommensurate (IC) magnetic structures (ICM), some of which exhibit ferroelectricity induced by frustrated magnetic orders.⁵⁻¹⁰ Their common phase sequence upon decreasing temperature T includes transitions from the high- T paramagnetic and paraelectric (PE) to an antiferromagnetic (AFM) but still PE phase at $T_{N1} \approx 44$ K, with an IC magnetic modulation along the orthorhombic a and c axes. At $T_{C1} \approx 39$ K, a lock-in transition takes place into a CM magnetic phase [$\vec{q} = (0.5, 0, 0.25)$], which is ferroelectric (FE). At lower temperature T_{C2} , all RMn_2O_5 compounds experience another transition where \vec{q} unlocks again into different IC values and the FE polarization shows a sharp drop (but not necessarily to zero). Additional changes of the magnetic order that are identified as spin reorientations in the CM phase have been reported for some RMn_2O_5 , for example DyMn_2O_5 (Ref. 9) and HoMn_2O_5 .¹¹ It is remarkable that all magnetic (and FE) phase transitions are clearly resolved in anomalies of the dielectric constant, the FE polarization, and the thermal expansivities, which proves the prominent role of the spin-lattice coupling in the multiferroic properties of these compounds.^{11,12} The origin of the phase complexity of RMn_2O_5 lies in the peculiarities of the lattice structure with different magnetic ions (Mn^{4+} , Mn^{3+} , rare earth) and a multitude of partially competing superexchange interactions, leading to a high degree of frustration in the magnetic system.⁷ In particular, the smallest loop of nearest-neighbor Mn ions with AFM exchange interactions in the a - b plane has five members, which naturally leads to geometric frustration of the Mn spins.¹¹ Frustrated systems are susceptible to small perturbations such as magnetic fields or pressure, since many

different magnetic structures are close in energy and compete for the ground state. For some RMn_2O_5 compounds it was recently demonstrated that the low-temperature IC phase is extremely sensitive to magnetic fields^{9,12-14} or to hydrostatic pressure.¹⁵ This opens not only new venues to mutually control magnetic and FE properties, but it also provides important insight into the microscopic interactions that are essential for the physics of multiferroic materials.

YMn_2O_5 is unique among all RMn_2O_5 compounds such that it experiences a FE polarization reversal at T_{C2} , which is the transition into the low- T IC phase.^{5,10} This effect was attributed to a change of the relative phase of the AFM orders of neighboring (a axis) chains of Mn^{3+} - Mn^{3+} - Mn^{4+} - Mn^{3+} - Mn^{3+} - Mn^{4+} ... spins based on an exchange striction mediated mechanism for the FE displacement of frustrated Mn^{3+} - Mn^{4+} spins between neighboring chains.^{3,10,11} However, recent experiments have detected a small deviation of the Mn spins from the a - b plane forming a noncollinear (spiral) modulation along the c axis in RMn_2O_5 multiferroics.¹⁶⁻¹⁹ This spiral-spin order also breaks the inversion symmetry^{3,20} and it was considered as an alternative mechanism for ferroelectricity in these compounds.^{16-18,21} The essential difference between the two proposed mechanisms is the microscopic nature of the exchange coupling that has to be involved. In the spin current (spiral) model,^{22,23} the weak antisymmetric Dzyaloshinskii-Moriya interaction ($\sim \vec{S}_i \times \vec{S}_j$) creates the magnetoelectric coupling, whereas in the exchange striction model, the FE polarization has its origin in the ionic displacements lifting the frustration of spins interacting via the symmetric exchange (or superexchange) interactions ($\sim \vec{S}_i \cdot \vec{S}_j$). Whether the spiral-spin model or the exchange striction model provides the better explanation of the FE order in the RMn_2O_5 compounds is still a matter of discussion^{24,25} and needs further explorations. In order to gain a deeper insight into the microscopic mechanisms of ferroelectricity of RMn_2O_5 , we have investigated the effect of hydrostatic pressure on the FE properties of YMn_2O_5 and found that the FE polarization in

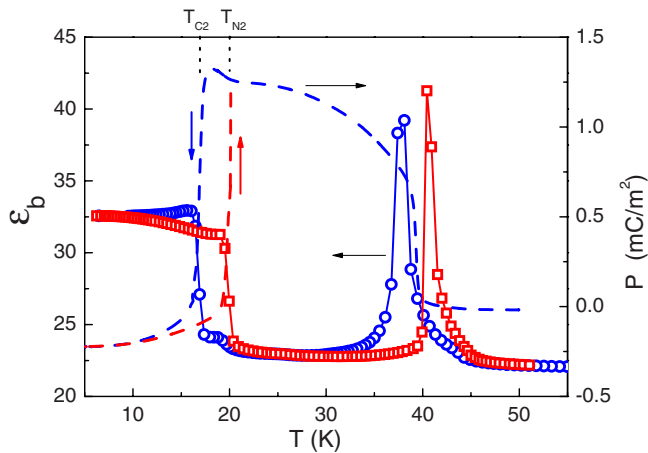


FIG. 1. (Color online) Dielectric constant (circles, decreasing T ; squares, increasing T) and ferroelectric polarization (dashed lines) of YMn_2O_5 . T_{N2} and T_{C2} are marked for decreasing T only.

the low-temperature IC phase ($T < T_{C2}$) reverses sign above a critical pressure. These data correlate with the lattice strain at T_{C2} measured by high-resolution thermal-expansion experiments. Our results are interpreted within the exchange striction model in terms of a pressure control of the relative phase of magnetic orders in neighboring AFM zigzag chains.

Single crystals of YMn_2O_5 grown from the flux were polished to thin platelets (0.2 mm thick) so that the dielectric constant and the pyroelectric current could be measured along the orthorhombic b axis. Hydrostatic pressure was applied employing a beryllium-copper clamp cell.¹⁵ A mixture of Fluorinert 70 and 77 liquids, was used as the pressure transmitting medium. Thermal-expansion measurements were conducted along the a , b , and c axes using a capacitance dilatometer. Since YMn_2O_5 exhibits a polarization reversal at T_{C2} , special care was taken to measure the FE polarization correctly in both FE phases above and below T_{C2} , respectively. Details of the experimental procedure are discussed elsewhere.²⁶

The dielectric constant and FE polarization at ambient pressure, shown in Fig. 1, is consistent with earlier reports,^{5,27,28} however, a careful investigation reveals subtle features that have to be discussed in more detail. Upon decreasing temperature, the dielectric constant shows a sudden increase at T_{N1} , the onset of sinusoidal IC magnetic order, and a sharp peak at the FE transition temperature T_{C1} , where the magnetic order locks into a CM modulation. The sharp increase in $\epsilon(T)$ at $T_{C2} \approx 17$ K indicates the unlocking of the magnetic modulation into the low- T IC phase. The FE polarization displays the corresponding increase at T_{C1} and drop at T_{C2} , respectively (Fig. 1). An additional small steplike anomaly of $\epsilon(T)$ at $T_{N2} \approx 19$ K, which is also reflected in a sudden change of slope of the FE polarization upon cooling, has not been reported before. It is similar to the more pronounced step of $\epsilon(T)$ observed in HoMn_2O_5 .¹¹ Note that our data for $P(T)$ confirm the sign change of the FE polarization at T_{C2} , although the value of $P(T)$ in the CM phase ($T_{C2} < T < T_{C1}$) is significantly different from earlier reports. This is due to the special procedure of poling the FE domains that is used in the present work, which provides a more accurate determination of $P(T)$.²⁶

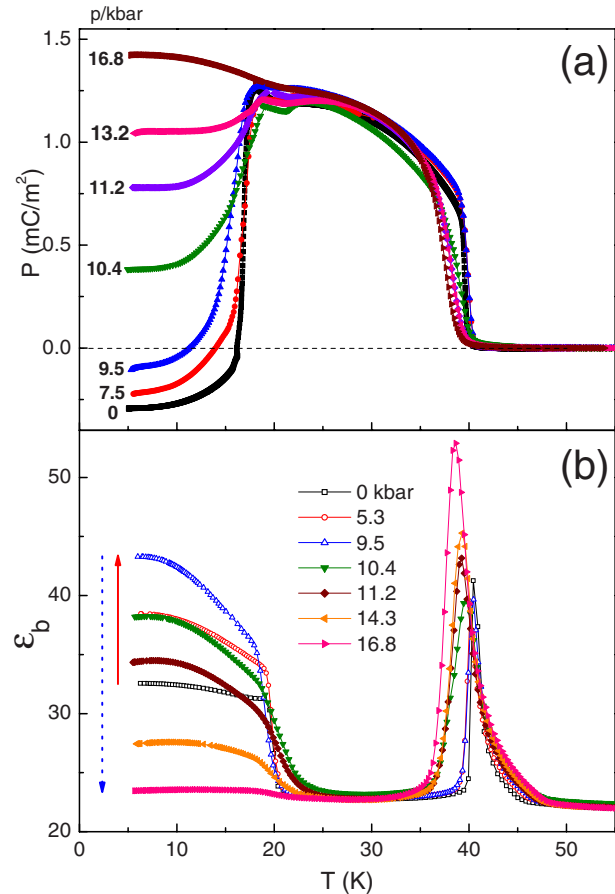


FIG. 2. (Color online) Temperature dependence of (a) the ferroelectric polarization and (b) the dielectric constant of YMn_2O_5 at different pressures.

With the application of hydrostatic pressure, the FE polarization P is dramatically altered at low temperatures [Fig. 2(a)]. At low pressure $P(T)$ increases slightly but it suddenly changes sign at a critical pressure of $p_c \approx 10$ kbar. After the sign reversal $P(T)$ increases quickly and approaches the FE polarization of the CM high-polarization phase. At T_{C2} a small drop of $P(T)$ is still visible up to 14 kbar, but it disappears completely at the highest pressure of this investigation (16.8 kbar), suggesting that the IC low-temperature phase is completely suppressed by pressures exceeding 14 kbar. The unique pressure-induced sign reversal of P has not been observed before and it needs a careful discussion of the magnetic structures and its relations to the FE order. The temperature dependence of the dielectric constant at various pressures [Fig. 2(b)] supports the conclusions derived from the polarization measurements. The sharp increase in $\epsilon(T)$ at T_{C2} is enhanced with the application of pressure up to about 10 kbar [indicated by the solid arrow in Fig. 2(b)]. However, above the critical pressure, $\epsilon(T)$ of the low- T IC phase suddenly decreases as the polarization changes sign [dotted arrow in Fig. 2(b)]. The pressure related changes of ϵ and P in the low- T IC phase are clearly visible in Fig. 3, showing both $\epsilon(5$ K) and $P(5$ K) as functions of pressure. The transition from negative to positive FE polarization happens in a narrow pressure range between 9.5 and 10.5 kbar. In the same pressure range $\epsilon(5$ K) experiences a sharp drop. It is inter-

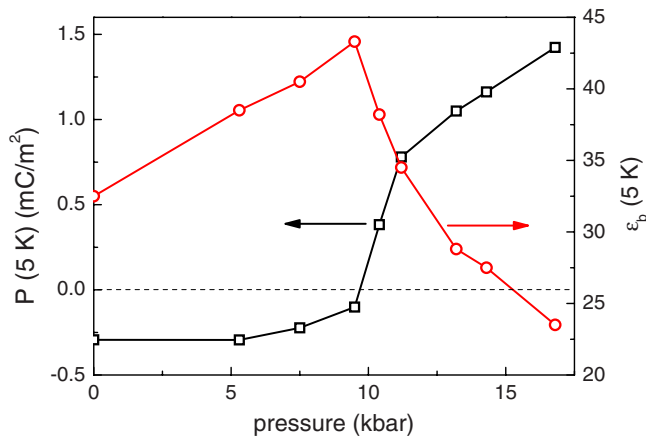


FIG. 3. (Color online) Dielectric constant and ferroelectric polarization of YMn_2O_5 at 5 K as a function of pressure.

esting that the phase transition at T_{C2} is only suppressed at a much higher pressure, suggesting that the sign change of the FE polarization (at 10 kbar) and the ICM \rightarrow CM transition (above 14 kbar) are two well-distinguished phenomena that have to be considered as separate transitions. The maximum of the low- T $\epsilon(p)$ in Fig. 3 indicates a softness of the lattice in response to the electric field right at the critical pressure where the magnetic structure shows a significant change. This is further evidence for the strong coupling of the spins to the lattice. When the magnetic system becomes less rigid at the transition, the lattice follows and the response to an electric field (dielectric constant) exhibits a maximum.

To understand the effect of external pressure on the ferroelectricity in YMn_2O_5 better, we investigated the subtle changes of the lattice at the various phase changes. While x-ray scattering experiments have not been successful in resolving the lattice strain at the FE transitions,²⁹ our high-resolution thermal-expansion measurements clearly show the abrupt change of the lattice constants at all magnetic and FE transitions (Fig. 4). Upon decreasing T , the a and c axes show a sudden increase at T_{N1} , whereas there is no anomaly in the b -axis length. This is associated with the onset of the

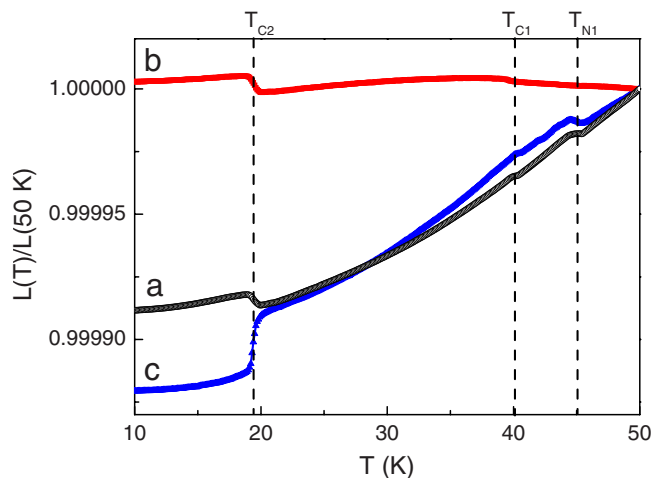


FIG. 4. (Color online) Temperature dependence of lattice constants of YMn_2O_5 below 50 K.

IC magnetic modulation along a and c . At the FE transition (T_{C1}) all three axes indicate a small increase as a signature of the onset of FE order and the locking into the CM magnetic phase. The largest expansion anomaly, however, is detected at T_{C2} , the low- T ICM \rightarrow CM transition where the FE polarization reverses sign. The relative changes of a , b , and c at T_{C2} are 9.3×10^{-6} , 7.1×10^{-6} , and -19.2×10^{-6} , respectively. While the volume change is small, the strain on the lattice parameters is significant, a and b expand while c shrinks in passing into the low- T IC phase. The similar change of the lattice constants at T_{C2} in other RMn_2O_5 crystals ($R = \text{Ho}, \text{Tb}$) (Ref. 11) imply the common origin of this typical lattice distortion, which is the partial release of the magnetic frustration between the a -axis zigzag chains.

The low- T CM \rightarrow ICM transition is supposedly driven by the increasing magnetic frustration between two adjacent Mn-spin chains along the a axis. The magnetic coupling between these two chains is mainly through the superexchange interactions between pairs of Mn^{3+} and Mn^{4+} spins via the neighboring oxygen ions. In the CM FE phase, following the zigzag chains along a , every second pair of spins is frustrated whereas the remaining pairs are not.^{7,10} With the decrease in temperature the magnitude of this frustration increases with the increase in the Mn sublattice magnetization and results in the phase transition at T_{C2} . There is a combination of magnetic and lattice effects involved. (i) The lattice distortion as verified by the expansion anomalies (Fig. 4) does modify the relevant exchange coupling constants. In particular, the in-plane expansion and the c -axis compression slightly increase the angle of the Mn^{3+} -O- Mn^{4+} superexchange coupling, decreasing the magnitude of the corresponding coupling constant (J_3 in the notation of Blake *et al.*⁷) and the associated spin frustration. The Mn ions of the frustrated pair are also displaced to further reduce their exchange energy.²⁹ (ii) According to neutron-scattering data^{7,10} the local spin orientation also changes dramatically in the low- T IC phase increasing the relative angle between the spins of two neighboring chains to about 40° .¹⁰ The large angle between the spin systems reduces the frustration further but it also decreases the overall coupling between the spin chains. (iii) As a consequence, the magnetic modulation of every second chain “slides” by increasing the relative phase with respect to the magnetic wave of adjacent chains.¹⁰ This change of phase results in a further decrease in both the magnetic frustration and the FE polarization, as e.g., in HoMn_2O_5 and TbMn_2O_5 , or even in a reversal of the polarization (with a decrease in magnitude) as in YMn_2O_5 . Simultaneously, the magnetic modulation along a and c unlock from their commensurate values and the low- T phase becomes incommensurate.

The application of pressure, as shown in Fig. 2, reverses the polarization and stabilizes the commensurate phase. This is obviously triggered by the compression of the a - b plane suggesting that the FE polarization could also be controlled by an in-plane strain induced in thin films of YMn_2O_5 on appropriate substrates at ambient pressures. At the first critical pressure of 10 kbar, the phase shift of the magnetic order in neighboring chains is reduced, which results in the reversal of the polarization from $P < 0$ to $P > 0$.¹⁰ However, the sudden drop of the $P(T)$ at T_{C2} still persists above 10 kbar and the polarization smoothly increases with raising pres-

sure. Only above the second critical pressure of 14 kbar does the IC phase become unstable and transform into the high-polarization commensurate phase.

These results provide convincing evidence for the dramatic effects of lattice strain and the strength of the spin-lattice coupling on the ferroelectricity in YMn_2O_5 . The data for YMn_2O_5 should be compared to similar data for HoMn_2O_5 .^{11,30} This is an excellent opportunity to reveal the potential role of the rare-earth moment in these compounds. While the ionic size of the Y^{3+} and Ho^{3+} ions is nearly identical, the major difference between both compounds is the existence of the Ho magnetic moment that is missing in YMn_2O_5 . The phase sequence of both compounds is surprisingly similar. Even the spin reorientation transition at T_{N2} in the commensurate phase, previously identified in HoMn_2O_5 ,¹¹ is evident in YMn_2O_5 in the form of the small step of $\varepsilon(T)$ and the increase in $P(T)$ at 20 K with decreasing T . The main difference between both compounds is the magnitude of the polarization drop at T_{C2} . In HoMn_2O_5 , the polarization decreases but remains positive, whereas in YMn_2O_5 , the drop is so large that P reverses sign in the

low- T IC phase. Within the exchange striction model the drop of $P(T)$ can be explained by the change of spin orientation in every second chain and by the phase shift between the magnetic modulation of neighboring chains. It appears conceivable that the presence of the Ho magnetic moments and their interaction with the Mn moments stiffens the Mn chain system and reduces the phase shift between adjacent chains. This explains the lesser degree of the polarization change at T_{C2} (still remaining positive) in HoMn_2O_5 as compared to YMn_2O_5 (sign reversal). Detailed neutron-scattering experiments on HoMn_2O_5 , similar to the investigation of YMn_2O_5 , are suggested to reveal the details of the magnetic orders in passing from the commensurate into the incommensurate phase at T_{C2} and to confirm our conclusions.

This work is supported in part by the T.L.L. Temple Foundation, the J. J. and R. Moores Endowment, and the State of Texas through TCSUH. Work at Rutgers was supported by the National Science Foundation under Contract No. NSF-DMR-0520471.

-
- ¹M. Fiebig, *J. Phys. D* **38**, R123 (2005).
²W. Eerenstein, N. D. Mathur, and J. F. Scott, *Nature (London)* **442**, 759 (2006).
³S.-W. Cheong and M. Nostrovoy, *Nat. Mater.* **6**, 13 (2007).
⁴C. N. R. Rao and C. R. Serrano, *J. Mater. Chem.* **17**, 4931 (2007).
⁵A. Inomata and K. Kohn, *J. Phys.: Condens. Matter* **8**, 2673 (1996).
⁶N. Hur, S. Park, P. A. Sharma, S. Guha, and S.-W. Cheong, *Phys. Rev. Lett.* **93**, 107207 (2004).
⁷G. R. Blake, L. C. Chapon, P. G. Radaelli, S. Park, N. Hur, S.-W. Cheong, and J. Rodriguez-Carvajal, *Phys. Rev. B* **71**, 214402 (2005).
⁸S. Kobayashi, T. Osawa, H. Kimura, Y. Noda, I. Kagomiya, and K. Kohn, *J. Phys. Soc. Jpn.* **73**, 1593 (2004).
⁹W. Ratcliff, V. Kiryukhin, M. Kenzelmann, S.-H. Lee, R. Erwin, J. Schefer, N. Hur, S. Park, and S.-W. Cheong, *Phys. Rev. B* **72**, 060407(R) (2005).
¹⁰L. C. Chapon, P. G. Radaelli, G. R. Blake, S. Park, and S.-W. Cheong, *Phys. Rev. Lett.* **96**, 097601 (2006).
¹¹C. R. dela Cruz, F. Yen, B. Lorenz, M. M. Gospodinov, C. W. Chu, W. Ratcliff, J. W. Lynn, S. Park, and S.-W. Cheong, *Phys. Rev. B* **73**, 100406(R) (2006).
¹²C. R. dela Cruz, B. Lorenz, Y. Y. Sun, C. W. Chu, S. Park, and S.-W. Cheong, *Phys. Rev. B* **74**, 180402(R) (2006).
¹³D. Higashiyama, S. Miyasaka, N. Kida, T. Arima, and Y. Tokura, *Phys. Rev. B* **70**, 174405 (2004).
¹⁴D. Higashiyama, S. Miyasaka, and Y. Tokura, *Phys. Rev. B* **72**, 064421 (2005).
¹⁵C. R. dela Cruz, B. Lorenz, Y. Y. Sun, Y. Wang, S. Park, S.-W. Cheong, M. M. Gospodinov, and C. W. Chu, *Phys. Rev. B* **76**, 174106 (2007).
¹⁶Y. Noda, H. Kimura, Y. Kamada, T. Osawa, Y. Fukuda, Y. Ishikawa, S. Kobayashi, Y. Wakabayashi, H. Sawa, N. Ikeda, and K. Kohn, *Physica B (Amsterdam)* **385-386**, 119 (2006).
¹⁷H. Kimura, Y. Kamada, Y. Noda, K. Kaneko, N. Metoki, and K. Kohn, *J. Phys. Soc. Jpn.* **75**, 113701 (2006).
¹⁸H. Kimura, S. Kobayashi, Y. Fukuda, T. Osawa, Y. Kamada, Y. Noda, I. Kagomiya, and K. Kohn, *J. Phys. Soc. Jpn.* **76**, 074706 (2007).
¹⁹C. Vecchini, L. C. Chapon, P. J. Brown, T. Chatterji, S. Park, S.-W. Cheong, and P. G. Radaelli, *Phys. Rev. B* **77**, 134434 (2008).
²⁰M. Mostovoy, *Phys. Rev. Lett.* **96**, 067601 (2006).
²¹J. Okamoto, D. J. Huang, C.-Y. Mou, K. S. Chao, H.-J. Lin, S. Park, S.-W. Cheong, and C. T. Chen, *Phys. Rev. Lett.* **98**, 157202 (2007).
²²H. Katsura, N. Nagaosa, and A. V. Balatsky, *Phys. Rev. Lett.* **95**, 057205 (2005).
²³I. A. Sergienko and E. Dagotto, *Phys. Rev. B* **73**, 094434 (2006).
²⁴J.-H. Kim, S.-H. Lee, S. I. Park, M. Kenzelmann, J. Schefer, J.-H. Chung, C. F. Majkrzak, M. Takeda, S. Wakimoto, S. Y. Park, S.-W. Cheong, M. Matsuda, H. Kimura, Y. Noda, and K. Kakurai, arXiv:0803.1123 (unpublished).
²⁵P. G. Radaelli, L. C. Chapon, A. Daoud-Aladine, C. Vecchini, P. J. Brown, T. Chatterji, S. Park, and S.-W. Cheong, arXiv:0803.3736 (unpublished).
²⁶R. P. Chaudhury, C. R. dela Cruz, B. Lorenz, Y. Y. Sun, C. W. Chu, S. Park, and S.-W. Cheong (unpublished).
²⁷S. Matsumoto, M. Tanaka, I. Kagomiya, K. Kohn, and S. Nakamura, *Ferroelectrics* **286**, 185 (2003).
²⁸I. Kagomiya, S. Nakamura, S. Matsumoto, M. Tanaka, and K. Kohn, *J. Phys. Soc. Jpn.* **74**, 450 (2005).
²⁹I. Kagomiya, S. Matsumoto, K. Kohn, Y. Fukuda, T. Shoubu, H. Kimura, Y. Noda, and N. Ikeda, *Ferroelectrics* **286**, 167 (2003).
³⁰C. R. dela Cruz, B. Lorenz, M. M. Gospodinov, and C. W. Chu, *J. Magn. Magn. Mater.* **310**, 1185 (2007).